Received January 1999
Revised June 1999
Accepted July 1999

Similarity solutions for hydromagnetic mixed convection heat and mass transfer for Hiemenz flow through porous media

Ali J. Chamkha and Abdul-Rahim A. Khaled
Department of Mechanical and Industrial Engineering, Kuwait University, Safat, Kuwait

Keywords *Heat transfer, Porous medium, Hydromagnetics, Convection*

Abstract *The problem of coupled heat and mass transfer by mixed convection in a linearly stratified stagnation flow (Hiemenz flow) in the presence of an externally applied magnetic field and internal heat generation or absorption effects is formulated. The plate surface is embedded in a uniform Darcian porous medium and is permeable in order to allow for possible fluid wall suction or blowing and has a power-law variation of both the wall temperature and concentration. The resulting governing equations are transformed into similarity equations for the case of linearly varying wall temperature and concentration with the vertical distance using an appropriate similarity transformation. These ordinary differential equations are then solved numerically by an implicit, iterative, finite-difference scheme. Comparisons with previously published work are performed and excellent agreement between the results is obtained. A parametric study of all involved parameters is conducted and a representative set of numerical results for the velocity and temperature profiles as well as the skin-friction parameter, local Nusselt number, and the local Sherwood number is illustrated graphically to elucidate interesting features of the solutions.*

Nomenclature

B_o = Magnetic induction
c_p = Specific heat of the fluid
C = Concentration at any point in the flow field
C_f = Local skin-friction coefficient
C_∞ = Concentration at the free stream function
C_w = Concentration at the wall
D = Mass diffusivity
f = Dimensionless stream function
g = Gravitational acceleration
G = Mixed convection parameter
h = Local convective heat transfer coefficient
h_m = Local mass transfer coefficient
K = Permeability of the porous medium
k_e = Effective thermal conductivity of the porous medium
Le = Lewis number
N = Buoyancy ratio
M = Square of the Hartmann number
Nu_x = Local Nusselt number
Pr = Prandtl number
Q = Dimensional internal heat generation or absorption coefficient
s = Dimensional stratification coefficient
S = Dimensionless stratification coefficient
Sh_x = Local Sherwood number
T = Temperature at any point in the flow field
T_w = Wall temperature
T_∞ = Free stream temperature
U_∞ = Free stream velocity
u = Vertical or x-component of velocity
v = Horizontal or y-component of velocity
v_w = Wall horizontal velocity
V_o = Dimensionless wall mass transfer coefficient

International Journal of Numerical Methods for Heat & Fluid Flow, Vol. 10 No. 1, 2000, pp. 94-115.

x = Vertical distance along the plate
y = Horizontal distance normal to the plate

Greek symbols

α_e = Effective thermal diffusivity of the porous medium
β_C = Concentration expansion coefficient
β_T = Thermal expansion coefficient
δ = Dimensionless internal heat generation or absorption coefficient
ϕ = Dimensionless concentration
η = Coordinate transformation
λ = Power-law index for both wall temperature and concentration
υ = Fluid kinematic viscosity
ψ = Dimensional stream function
θ = Dimensionless temperature
ρ = Fluid density
σ = Fluid electrical conductivity
Ω = Porous medium parameter

Introduction

Stagnation flows are found in many applications such as flows over the tips of rockets, aircrafts, submarines and oil ships. The study of the stagnation flow problem was started by Hiemenz (1911) who developed an exact solution to the Navier-Stokes governing equations for the forced convection case. Later, Eckert (1942) studied a similar solution for both the momentum and energy governing equations excluding the effect of buoyancy forces.

Sparrow *et al.* (1962) have considered the effect of blowing and magnetic field on the heat transfer characteristics at the stagnation point on a vertical plate. Recently, Ariel (1994) has considered the stagnation point flow of electrically-conducting fluids in the presence of larger transverse magnetic field strengths than those used by Sparrow *et al.* (1962). Yih (1998) has reported on the effects of uniform suction/blowing and magnetic field on the heat transfer characteristics of the Hiemenz problem in porous media.

Simultaneous heat and mass transfer from different geometries embedded in porous media has many engineering and geophysical applications such as geothermal reservoirs, drying of porous solids, thermal insulation, enhanced oil recovery, packed-bed catalytic reactors, cooling of nuclear reactors, and underground energy transport. Cheng and Minkowycz (1977) have used the Darcy law in their study on free convection about a vertical impermeable flat plate in porous media. The problem of a vertical cylinder embedded in porous media has been investigated by Minkowycz and Cheng (1976) using the local non-similarity method and by Kumari *et al.* (1985) using the finite difference and improved perturbation methods. Some studies which considered coupled heat and mass transfer include the works of Gebhart and Pera (1971) on vertical plates, Pera and Gebhart (1972) and Chen and Yuh (1980) on inclined plates. Also, Lai (1991) has investigated coupled heat and mass transfer by mixed convection from an isothermal vertical plate in a porous medium and Yih (1997) has studied the effect of transpiration on the problem of Lai (1991).

There has been a renewed interest in studying magnetohydrodynamic (MHD) flow and heat transfer in porous and non-porous media due to the effect of magnetic fields on the performance of many systems using electrically-conducting fluids. For example, Raptis *et al.* (1982) have analyzed hydromagnetic free convection flow through a porous medium between two parallel plates. Aldoss *et al.* (1995) have studied mixed convection from a vertical plate

embedded in a porous medium in the presence of a magnetic field. Chamkha (1997a) has considered MHD free convection from a vertical plate embedded in a thermally-stratified porous medium with Hall effects.

In certain porous media applications such as those involving heat removal from nuclear fuel debris, underground disposal of radioactive waste material, storage of food stuffs, and exothermic chemical reactions in packed-bed reactors, the working fluid heat generation (source) or absorption (sink) effects are important. Representative studies dealing with these effects have been reported by such authors as Acharya and Goldstein (1985), Vajravelu and Nayfeh (1992) and Chamkha (1996,1997b).

The objective of this paper is to consider simultaneous heat and mass transfer of an electrically-conducting fluid by mixed convection in a stagnation flow over a flat plate embedded in a porous medium in the presence of fluid wall blowing or suction, magnetic field effects and temperature-dependent heat generation or absorption effects. This will be done for power-law variations of both the wall temperature and concentration and a linearly stratified free stream temperature.

Problem formulation

Consider steady, laminar, hydromagnetic coupled heat and mass transfer by mixed convection flow in front of a stagnation point on a vertical flat plate embedded in a porous medium. Both the temperature and concentration of the surface vary with the distance along the plate according to a power-law model and they are always greater than their free stream values existing far from the plate surface. The free stream temperature is assumed to be linearly stratified while the free stream concentration is assumed to be constant. A magnetic field of constant strength Bo is applied in the y-direction which is normal to the flow direction.

A constant fluid suction or blowing is imposed at the plate surface (see Figure 1). The fluid is assumed to be Newtonian, electrically conducting, heat generating or absorbing and has constant properties except the density in the buoyancy term of the balance of linear momentum equation. The magnetic

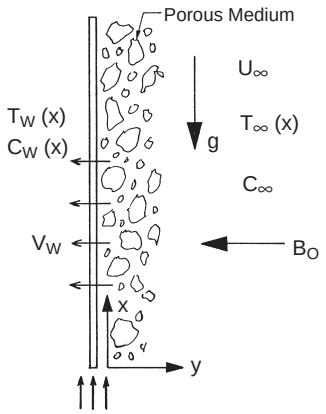

Figure 1.
Physical geometry and coordinate system

Reynolds number is assumed to be small so that the induced magnetic field can be neglected. In addition, there is no applied electric field and all of the Hall effect, viscous dissipation and Joule heating are neglected. Invoking the Boussinesq and boundary-layer approximations, the governing equations for this problem can be written as

$$\frac{\partial u}{\partial x} + \frac{\partial v}{\partial y} = 0 \tag{1}$$

$$\begin{aligned} u\frac{\partial u}{\partial x} + \frac{\partial u}{\partial y} &= \upsilon\frac{\partial^2 u}{\partial y^2} + U_\infty\frac{dU_\infty}{dx} + \beta_T g(T - T_\infty) + \beta_c g(C - C_\infty) \\ &\frac{-\sigma B_o^2}{\rho}(u - U_\infty) - \frac{\upsilon}{K}(u - U_\infty) \end{aligned} \tag{2}$$

$$\rho c_p\left(u\frac{\partial T}{\partial x} + v\frac{\partial T}{\partial y}\right) = k_e\frac{\partial^2 T}{\partial y^2} + Q(T - T_\infty) \tag{3}$$

$$u\frac{\partial C}{\partial x} + v\frac{\partial C}{\partial y^2} = D\frac{\partial^2 C}{\partial y^2} \tag{4}$$

where u, v, T and C are the fluid x-component of velocity, y-component of velocity, temperature, and concentration, respectively. $\rho, \upsilon, c_p, \beta_T,$ and β_c are the fluid density, kinematic viscosity, specific heat at constant pressure, coefficient of thermal expansion, and coefficient of concentration expansion, respectively. σ, Q and D are the fluid electrical conductivity, heat generation (> 0) or absorption (< 0) coefficient, and mass diffusivity, respectively. K, g and B_o are the permeability of the porous medium, gravitational acceleration and magnetic induction, respectively. k_e, U_∞, T_∞ and C_∞ are the porous medium effective thermal conductivity, and the fluid free stream velocity, temperature and concentration, respectively.

The above described problem has the following boundary conditions:

$$\begin{aligned} &u(x,0) = 0, \quad v(x,0) = -v_w, \quad T(x,0) = T_w, \quad C(x,0) = C_w \\ &u(x,\infty) = U_\infty = Ax, \quad T(x,\infty) = T_\infty, \quad C(x,\infty) = C_\infty \end{aligned} \tag{5}$$

where A is a constant and v_w, T_w and C_w are the suction (> 0) or injection (< 0) velocity and the fluid temperature and concentration at the plate, respectively. Both the wall temperature and concentration are assumed to have power-law variation forms while the free stream temperature is linearly stratified with x as shown by the following equations:

$$T_w = T_\infty + c_1 x^\lambda, C_w = C_\infty + c_2 x^\lambda, T_\infty = T_o + sx \tag{6}$$

where c_1, c_2 and T_o are constants and "λ" is the power index of the wall temperature and concentration. It should be noted that both the wall temperature and concentration are assumed to have the same power index λ.

Defining the stream function Ψ such that $u = \partial\Psi/\partial y$ and $v = -\partial\Psi/\partial x$ and introducing the similarity variables employed earlier by Yih (1998) gives

$$\eta = \sqrt{\frac{A}{\alpha_e}}y, \Psi(x,y) = xf(\eta)\sqrt{A\alpha_e}, \theta(\eta) = \frac{T - T_\infty}{T_w - T_\infty}, \theta(\eta) = \frac{C - C_\infty}{C_w - C_\infty} \quad (7)$$

where α_e is the effective thermal diffusivity of the porous medium ($\alpha_e = k_e/(\rho c_p)$). Substituting equations (7) into equations (2) through (4) produces the following local similarity equations:

$$Prf''' + ff'' - f'^2 + 1 + (\Omega + M)(1 - f') + G(\theta + N\phi) = 0 \quad (8)$$

$$\theta'' + f\theta' - \lambda f'\theta + \delta\theta - Sf' = 0 \quad (9)$$

$$\frac{1}{Le}\phi'' + f\phi' - \lambda f'\phi = 0 \quad (10)$$

where a prime denotes ordinary differentiation with respect to η and

$$\begin{aligned} Pr &= \frac{\upsilon}{\alpha_e}, \quad Le = \frac{\alpha_e}{D}, \quad \delta = \frac{Q}{A\rho c_p}, \quad \Omega = \frac{\alpha_e}{KA}, \quad M = \frac{\sigma B_o^2}{\rho A} \\ G &= \frac{g\beta_T(T_w - T_\infty)}{AU_\infty}, \quad N = \frac{\beta_c(C_w - C_\infty)}{\beta_T(T_w - T_\infty)}, \quad S = \frac{T_\infty - T_o}{T_w - T_\infty} \end{aligned} \quad (11)$$

are the Prandtl number of the fluid, the Lewis number, the dimensionless internal heat generation or absorption coefficient, the dimensionless porous medium parameter, the magnetic parameter (square of the Hartmann number), the mixed convection parameter, the buoyancy ratio and the dimensionless stratification coefficient. Note that by allowing both the wall temperature and concentration to have similar power-law indices, N will always be constant. To eliminate the dependence of G and S on x and, therefore, obtain similarity equations, λ must be equal to unity. Accordingly, for the case of $\lambda = 1$ where all of wall temperature and concentration and free stream temperature and velocity are linearly changing with the vertical distance x along the vertical plate, the governing equations reduce to

$$Prf''' + ff'' - f'^2 + 1 + (\Omega + M)(1 - f') + G(\theta + N\phi) = 0 \quad (12)$$

$$\theta'' + f\theta' - f'\theta + \delta\theta - Sf' = 0 \quad (13)$$

$$\frac{1}{\mathrm{Le}}\phi'' + \mathrm{f}\phi' - \mathrm{f}'\phi = 0 \tag{14}$$

where $\mathrm{G} = \mathrm{g}\beta_{\mathrm{T}}\mathrm{c}_1/\mathrm{A}^2$ and $\mathrm{S} = \mathrm{s}/\mathrm{c}_1$. Equations (12) through (14) are similar equations.

Upon using equations (7), the dimensionless transformed boundary conditions become

$$\begin{aligned} &\mathrm{f}'(0) = 0, \quad \mathrm{f}(0) = \mathrm{V_o}, \quad \theta(0) = 1, \quad \phi(0) = 1 \\ &\mathrm{f}'(\infty) = 1, \quad \theta(\infty) = 0, \quad \phi(\infty) = 0 \end{aligned} \tag{15}$$

where $\mathrm{V_o} = \mathrm{v_w}/(\mathrm{A}\alpha_{\mathrm{e}})^{1/2}$ is the dimensionless wall normal velocity such that $\mathrm{V_o} > 0$ indicates suction and $\mathrm{V_o} < 0$ indicates blowing at the surface.

In the absence of mass diffusion (equation (10) is absent), and eliminating the effects of buoyancy (G = 0), heat generation or absorption (δ = 0) and thermal stratification (S = 0), equations (8), (9) and (15) reduce to

$$\mathrm{Prf}''' + \mathrm{ff}'' - \mathrm{f}'^2 + 1 + (\Omega + \mathrm{M})(1 - \mathrm{f}') = 0 \tag{16}$$

$$\theta'' + f\theta' - \lambda f'\theta = 0 \tag{17}$$

$$\begin{aligned} &\mathrm{f}'(0) = 0, \quad \mathrm{f}(0) = \mathrm{V_o}, \quad \theta(0) = 1, \\ &\mathrm{f}'(\infty) = 1, \quad \theta(\infty) = 0 \end{aligned} \tag{18}$$

which are exactly the same as those reported by Yih (1998). In addition, as $\Omega \to \infty$ and $\lambda = 1$ in equations (16) and (17), the following equations result

$$f' = 1 \tag{19}$$

$$\theta'' + \mathrm{f}\theta' - \mathrm{f}'\theta = 0 \tag{20}$$

Equations (19) and (20) subject to the boundary conditions (18) represent the problem of pure Darcy flow solved previously by Lai and Kulacki (1990).

Of special importance for this flow and heat transfer situation are the skin-friction parameter, local Nusselt number, and the local Sherwood number. These are defined as follows

$$\mathrm{SFP} = \frac{\mathrm{C_f}}{2}\sqrt{\mathrm{Re_x}} = \mathrm{f}''(0)\sqrt{\mathrm{Pr}} \tag{21}$$

$$\mathrm{Nu_x} = \frac{\mathrm{hx}}{\mathrm{k}} = -\theta'(0)\sqrt{\mathrm{Pe_x}} \tag{22}$$

$$\mathrm{Sh_x} = \frac{\mathrm{h_m x}}{\mathrm{D}} = -\phi'(0)\sqrt{\mathrm{Pe_x}} \tag{23}$$

where C_f, Re_x, h, h_m and Pe_x are the skin friction coefficient at any point near the stagnation point on the wall, local Reynolds number ($Re_x = U_\infty x/\upsilon$), local convective heat transfer coefficient, the local mass transfer coefficient and the local Peclet number ($Pe_x = U_\infty x/\alpha_e$), respectively.

Numerical method

The implicit finite-difference method discussed by Blottner (1970) is employed in the present work because of its simplicity and its reliable results especially for equations and boundary conditions having forms similar to equations (8) through (15). Equation (12) is a third-order differential equation which is reduced to a second-order one by letting $V = f'$. Then, all second-order differential equations are linearized and then descritized using three-point central difference quotients with variable step sizes in the h direction. The resulting equations form a tridiagonal system of algebraic equations that can be solved by the well-known Thomas algorithm (see Blottner, 1970). After that, the first-order equation $V = f'$ is then solved for f using the trapezoidal rule. Owing to the non-linear nature of the equations, an iterative procedure is employed. For convergence, the maximum absolute error between two successive iterations was taken to be 10^{-7}. After many numerical experimentations performed to assess solution grid-size independence, a starting step size of 0.001 in the η direction with an increase of 1.015 times the previous step size was found to give accurate results for all the range of physical parameters. The total number of points in the η direction was taken to be 499 to ensure proper approach of the solution to the free stream conditions. Tables I-IV present comparisons between the solutions obtained by the aforementioned numerical method for special cases of the local-similar equations and those obtained by different authors as shown below. It is found that the results of the present work are in excellent agreement with the other available published results. This lends confidence in the numerical results to be reported subsequently.

Results and discussion

Figures 2 and 3 present the trend of the velocity and the temperature profiles for the cases represented in Table V with all of S, M being set to zero and λ being equal to unity. The decrease in the Prandtl number from Pr = 10 to Pr = 1 has been shown to produce a large increase in the velocity due to both buoyancy effect and decreased viscosity. These have the direct effect of reducing the temperature when Pr = 1 as shown from curves I and II in Figures 2 and 3.

Increasing the tightness of the porous medium which is represented by increases in Ω results in increasing the resistance against the flow. Thus, the velocity decreases and the temperature increases as shown from curve III compared to curve I in both Figures 2 and 3. Application of a magnetic field

M	$v_o = -1$			$v_o = 0$				$v_o = 1$	
	Sparrow *et al.* (1962)	Yih (1998)	Present work	Sparrow *et al.* (1962)	Ariel (1994)	Yih (1998)	Present work	Yih (1998)	Present work
0	0.7605	0.75658	0.75689	1.231	1.23259	1.23259	1.23290	1.88931	1.88890
1	1.124	1.11642	1.11634	1.584	1.58533	1.58533	1.58494	2.20294	2.20164
4	1.892	1.87762	1.87633	2.345	2.34666	2.34666	2.34457	2.92011	2.91669
25	–	4.66753	4.65705	–	5.14796	5.14796	5.13521	5.67683	5.66130
100	–	9.58591	9.54054	–	10.0747	10.0747	10.0246	10.5884	10.5330

Table I.
Comparison of the values of SFP for various values of M and V_o with $G = 0$, $Pr = 1$, $S = 0$, $\Omega = 0, \lambda = 0$ and $\delta = 0$

Pr	Sparrow *et al.* (1962)	Evans (1962)	$\lambda = 0$ Lin and Lin (1987)	Yih (1998)	Present work	$\lambda = 1$ Yih (1998)	Present work
0.0001	–	0.007938	0.007938	0.007938	0.008058	0.012433	0.012506
0.001	–	0.024829	0.024829	0.024829	0.025203	0.038658	0.038885
0.01	0.07596	0.075972	0.075973	0.075973	0.077091	0.116372	0.117049
0.1	0.2194	0.219503	0.219505	0.219503	0.222560	0.324927	0.326747
1	0.5705	0.570466	0.570466	0.570465	0.577689	0.811301	0.815499
10	1.349	1.33880	1.33880	1.338796	1.354430	1.861577	1.870514
100	–	2.98633	2.98634	2.986329	3.019810	4.115021	4.134014
1,000	–	6.52914	6.52914	6.529137	6.601049	8.963783	9.004434
1,0000	–	14.158	14.1583	14.158301	14.313023	19.408995	19.494321

Table II.
Comparison of the values of $Nu_x Re_x^{-1/2}$ for various values of Pr and λ with $G = 0$, $M = 0$, $S = 0$, $V_o = 0$, $\Omega = 0$ and $\delta = 0$

V_o	Lai and Kulacki (1990)	Yih (1998)	Present work
–1	0.7766	0.776625	0.778149
–0.5	0.9909	0.990908	0.992572
0	1.2533	1.253298	1.254966
0.5	1.5599	1.559856	1.561175
1	1.9043	1.904254	1.905056

Table III.
Comparison of the values of $Nu_x Pe_x^{-1/2}$ for various values of V_o with $G = 0$, $M = 0$, $Pr = 1$, $S = 0$, $\lambda = 1$, $\Omega = 10^{10}$ and $\delta = 0$

produces a resistive force called the Lorentz force which has the same effect as that of the porous medium parameter Ω. For this reason no results will be shown for various values of the magnetic parameter M which has the physical range $0 \leq M \leq 100$. Curve VII shows the effect of the internal heat generation on both the velocity and temperature profiles. Heat generation increases the fluid temperature and, consequently, it increases the thermal buoyancy forces (if present) which, in turn, increases the velocity of the flow.

Including the mass diffusion effects increases the flow velocity and decreases its temperature due to additional concentration buoyancy forces. This is obvious from curves IV and V which correspond to different Lewis numbers compared to curve I in which the concentration buoyancy forces are eliminated by setting N equal to zero. Surface suction keeps the boundary layer more attached to the wall and this has an effect of decreasing the temperature as shown from curve VI compared to curve I in Figure 3.

Figures 4 and 5 present the effect of the Prandtl number Pr and the porous medium parameter Ω on the local skin-friction coefficient $SFP/Pr^{1/2}$ and the Nusselt number as a function of the flow Reynolds number ($Nu_x Re_x^{-1/2}$) instead of its Peclet number, respectively.

Ω	$\lambda = 0$ Yih (1998)	$\lambda = 0$ Present work	$\lambda = 1$ Yih (1998)	$\lambda = 1$ Present work
0	0.570465	0.570465	0.811301	0.815499
10^{-4}	0.570468	0.572804	0.811307	0.812658
10^{-3}	0.570497	0.572833	0.811355	0.812706
10^{-2}	0.570782	0.573120	0.811833	0.813185
10^{-1}	0.573556	0.575904	0.816490	0.817842
1	0.595346	0.597787	0.853324	0.854695
10	0.668343	0.671200	0.981856	0.983427
10^{2}	0.742746	0.746169	1.127734	1.129389
10^{3}	0.778644	0.782388	1.207239	1.209454
10^{4}	0.791608	0.795471	1.237983	1.240297
10^{5}	0.795880	0.799768	1.248385	1.250696
10^{6}	0.797249	0.801099	1.251747	1.253948
10^{7}	0.797683	0.801437	1.252818	1.254775
10^{8}	0.797821	0.801490	1.253157	1.254904
10^{9}	0.797864	0.801495	1.253264	1.254918
∞	0.797885	0.801496	1.253298	1.254966

Table IV.
Comparison of the values of $Nu_x Pe_x^{-1/2}$ for various values of Ω and λ with $G = 0$, $M = 0$, $Pr = 1$, $S = 0$, $V_o = 0$ and $\delta = 0$

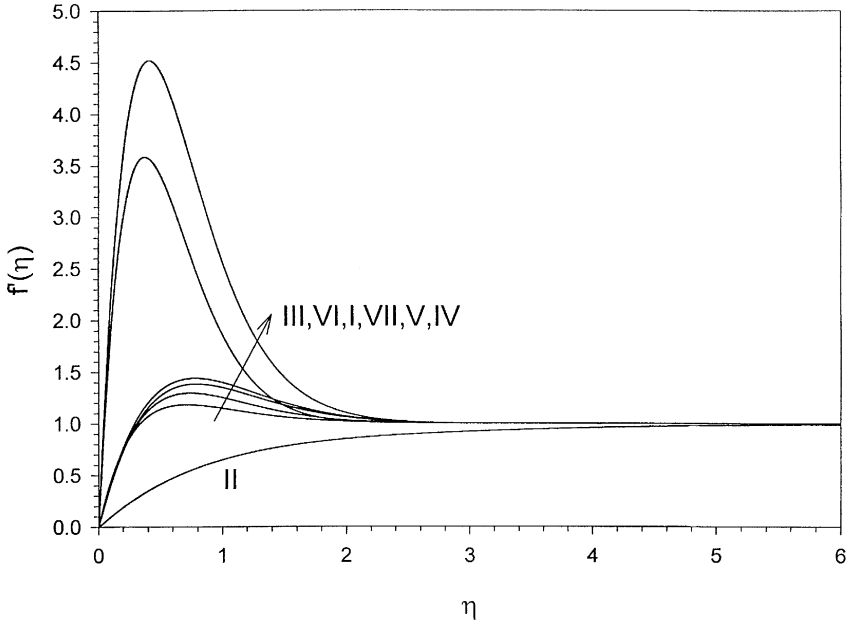

Figure 2.
A parametric study for velocity profiles

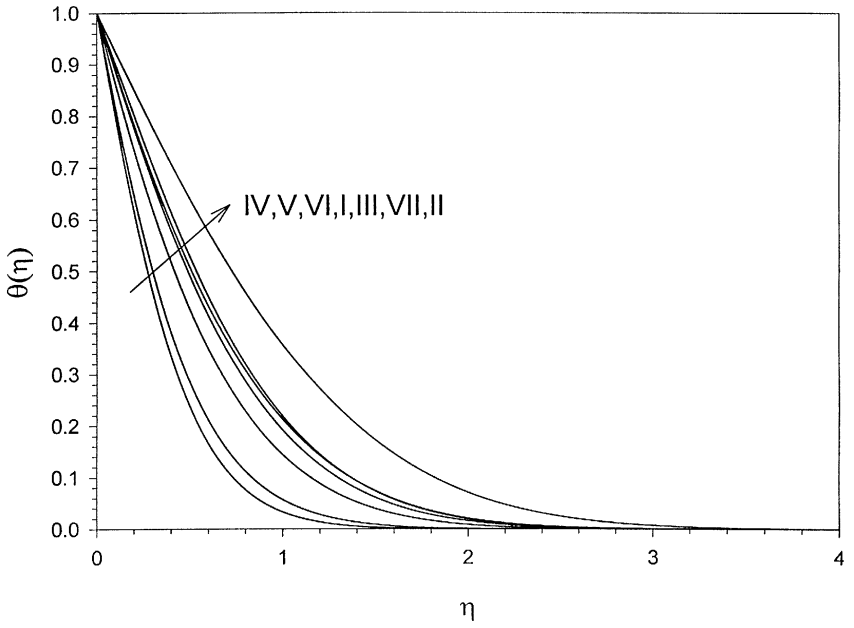

Figure 3.
A parametric study for temperature profiles

Curve	Pr	Ω	G	N	V_o	Le	δ
I	1	0.0001	10	0	0	0.5	0
II	10	0.0001	10	0	0	0.5	0
III	1	10	10	0	0	0.5	0
IV	1	0.0001	10	10	0	0.5	0
V	1	0.0001	10	10	0	1.25	0
VI	1	0.0001	10	0	0.5	0.5	0
VII	1	0.0001	10	0	0	0.5	0.5

Table V.
Parametric values for the curves in Figures 1 and 2 (M = 0, S = 0 and ∞ = 1)

Increases in the values of Pr result in decreases in the flow temperature and its absolute slope at the wall. This results in enhancements in the values of the local Nusselt number as shown in Figure 5. In Figure 4, the skin-friction parameter is presented in the same way as done by Yih (1998). This Figure shows that $SFP/Pr^{1/2}$ decreases with increasing values of Pr. Also, while the values of $SFP/Pr^{1/2}$ change considerably as Pr changes from 0.01 and 0.7, they do not vary as much for higher values of (Pr = 6.7 and Pr = 10). It is worth noting that when SFP and $Nu_xPe_x^{-1/2}$ are plotted instead of $SFP/Pr^{1/2}$ and $Nu_xPe_x^{-1/2}$, the effect of Pr on the skin-friction parameter is observed to be appreciable only for large values of Ω and the local Nusselt number as a function of the flow Peclet number becomes independent of the Prandtl number as $\Omega \rightarrow \infty$ and approaches a constant value of 1.254966.

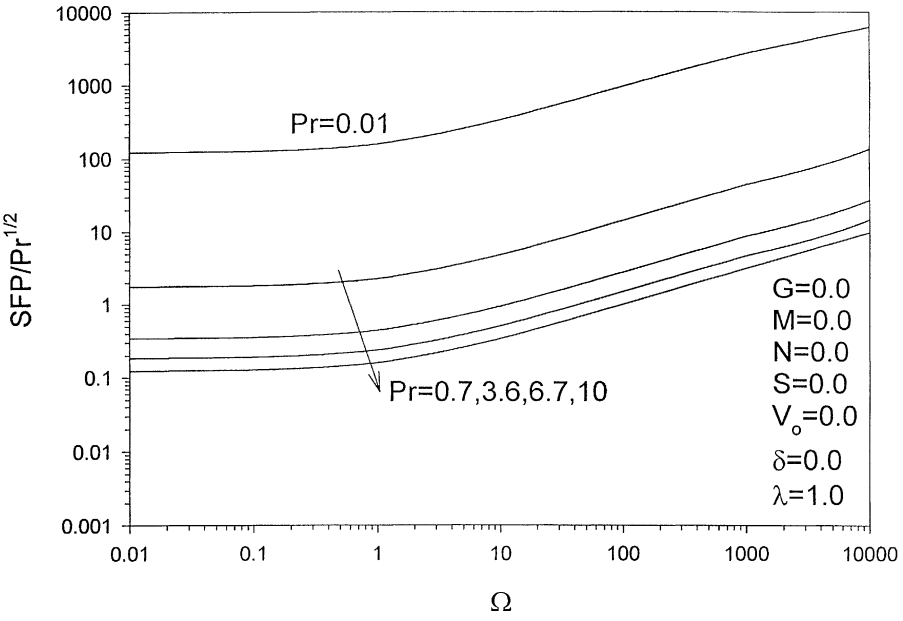

Figure 4.
Effects of Pr and Ω on the skin-friction parameter

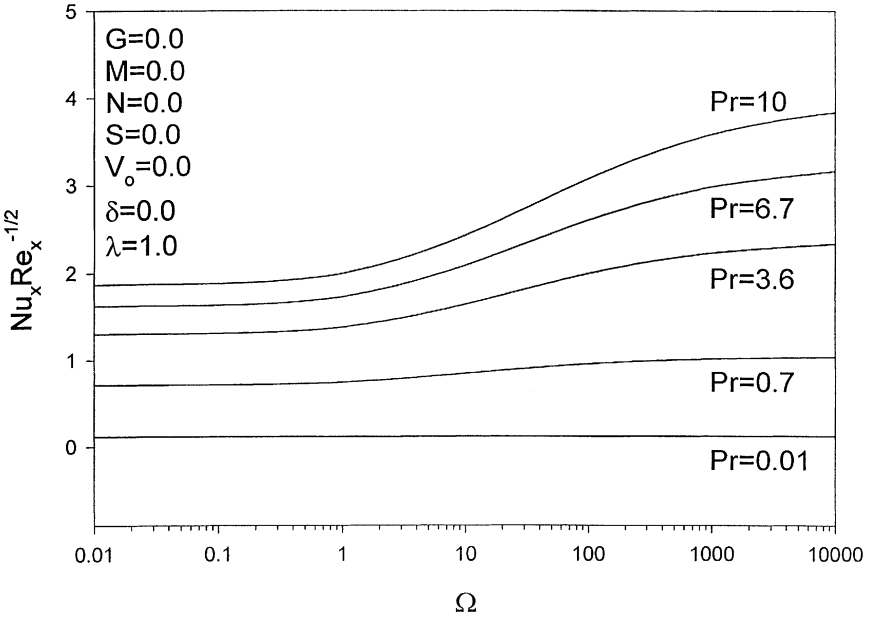

Figure 5.
Effects of Pr and Ω on the local Nusselt number

Figures 6 and 7 show the effect of the stratification coefficient S and the dimensionless porous medium parameter Ω on the skin-friction parameter and the local Nusselt number, respectively. The value of S = –1 results in no heat transfer since it requires that the wall temperature equals to the free stream temperature at any distance from the stagnation point.

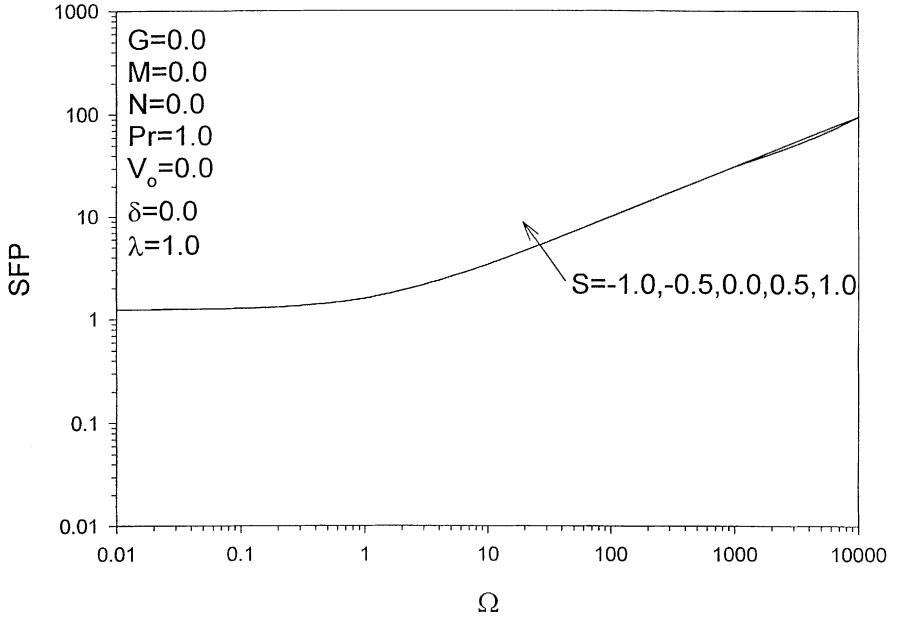

Figure 6.
Effects of S and Ω on the local skin-friction parameter

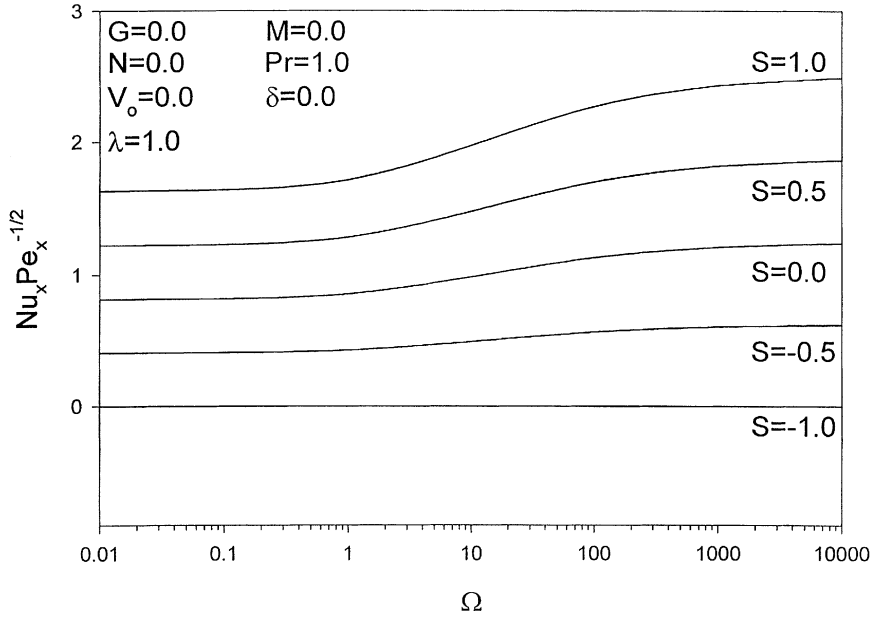

Figure 7.
Effects of S and Ω on the local Nusselt number

As expected, in the absence of the buoyancy effects (G = 0), the increase in S has no effects on the skin-friction parameter. However, it enhances the wall heat transfer because of the expected increase in the wall and the free stream temperature gradients along the x-direction which causes increases in the convective heat transfer as shown in Figures 6 and 7, respectively.

Figures 8 and 9 depict the effect of the mixed convection parameter G and the porous medium parameter Ω on the values of SFP and $Nu_x Pe_x^{-1/2}$, respectively. As G increases, the buoyancy force near the stagnation point increases. Hence, the flow velocity increases causing increases in the values of

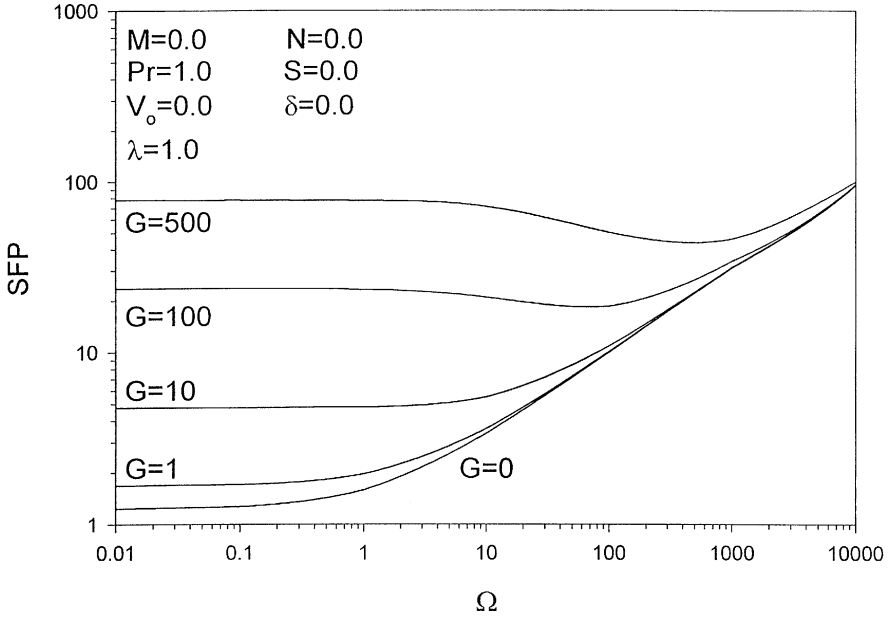

Figure 8.
Effects of G and Ω on the skin-friction parameter

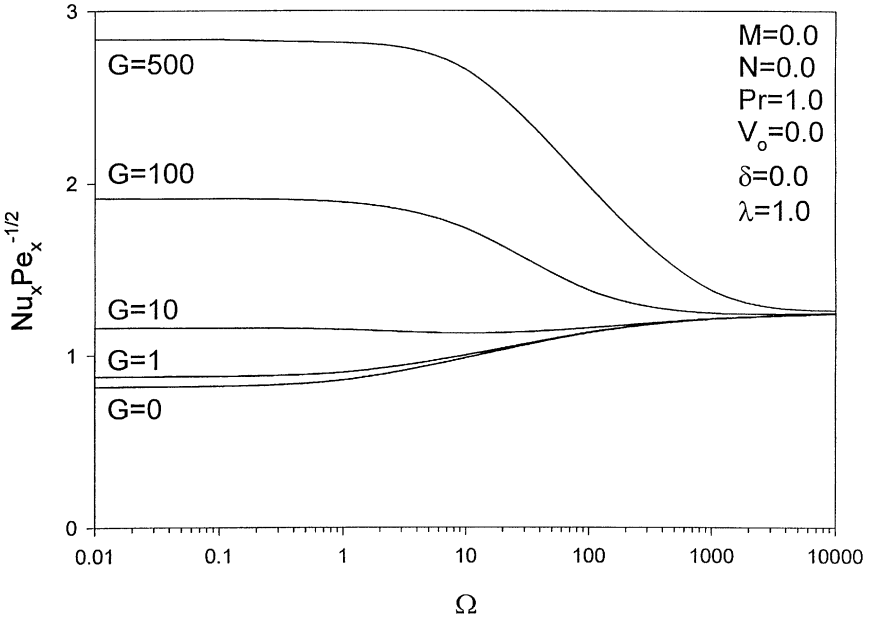

Figure 9.
Effects of G and Ω on the local Nusselt number

SFP and accordingly, the values of the local Nusselt number increase, as is evident from Figures 8 and 9, respectively. It should be mentioned that the effect of the buoyancy force is absent for large values of Ω, as is evident from the previous Figures.

Figures 10 and 11 display the effects of the dimensionless internal heat generation or absorption coefficient δ and Ω on the skin-friction parameter and the local Nusselt number, respectively. As seen from Figure 3, heat generation enhances the fluid temperature and its gradient at the wall as well as the wall slope of the velocity profile. This results in decreasing the values of the local Nusselt number and increasing the values of SFP as shown in Figures 11 and 10, respectively. The effect of δ on SFP is more pronounced for small values of Ω than for larger ones as shown in Figure 10.

Figures 12-15 illustrate the effects of the buoyancy ratio N and the Lewis number Le on the skin-friction parameter and the local Nusselt and Sherwood numbers, respectively. Again, one can notice from Figure 3 that the absolute wall temperature slope is increased as a result of increasing N and decreasing Le. This causes enhancements in the values of the local Nusselt number and similarly for the local Sherwood number since the energy and concentration equations have the same form. These behaviours can be seen from Figure 13. However, increases in the values of Le cause reductions in the values of the local Nusselt number and increases in the values of the local Sherwood number as shown in Figures 14 and 15. Also, it is noticed from Figure 2 that the wall slope of velocity is increased as N is increased. Therefore, the skin-friction parameter SFP increases as N increases as is shown in Figure 12.

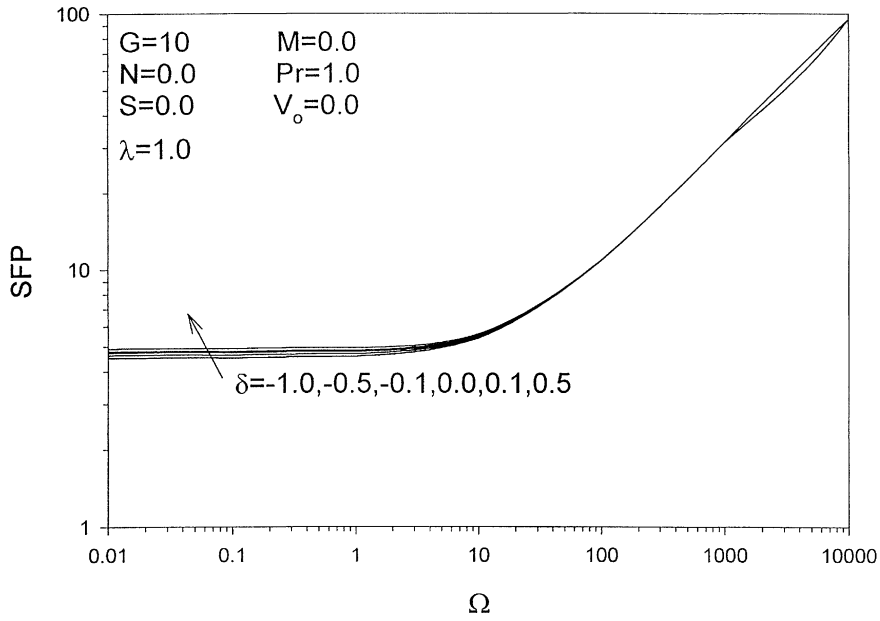

Figure 10.
Effects of δ and Ω on the skin-friction parameter

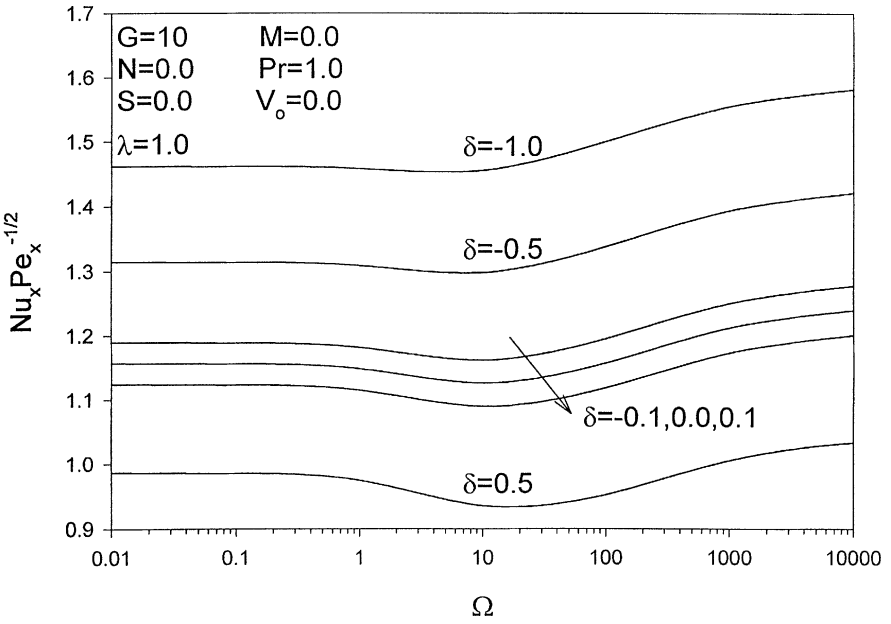

Figure 11.
Effects of δ and Ω on the local Nusselt number

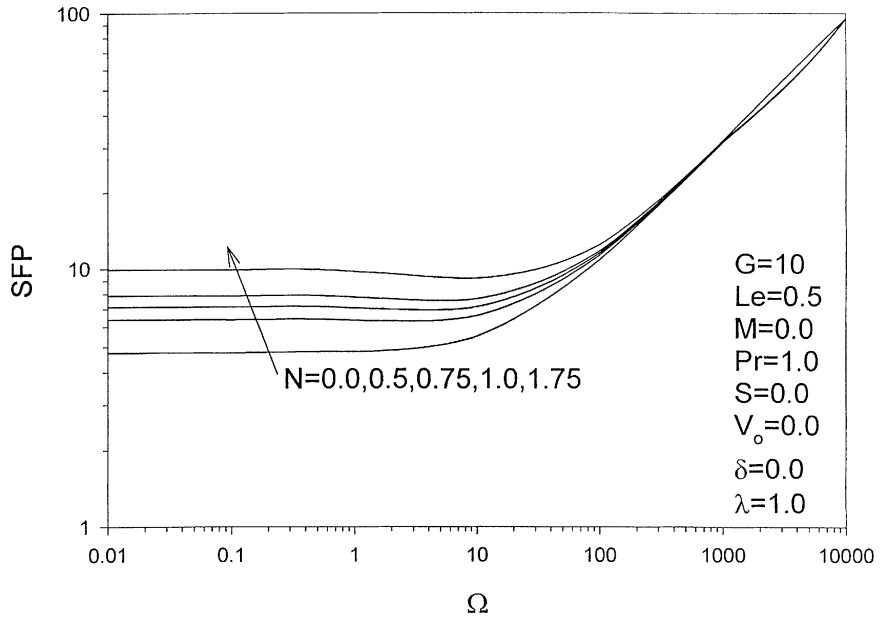

Figure 12.
Effects of N and Ω on the skin-friction parameter

In Figures 16 and 17, the effects of the wall mass transfer coefficient or dimensionless normal velocity V_o and Ω on the skin-friction parameter and the local Nusselt number are explained, respectively. Surface fluid injection effects, when V_o is less than zero, tend to increase the velocity boundary layer. This has

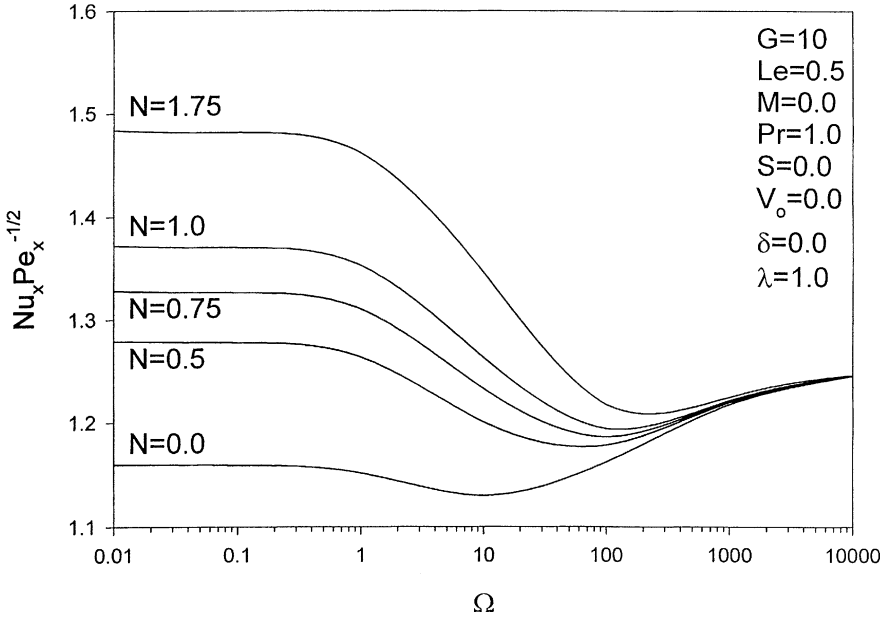

Figure 13.
Effects of N and Ω on the local Nusselt number

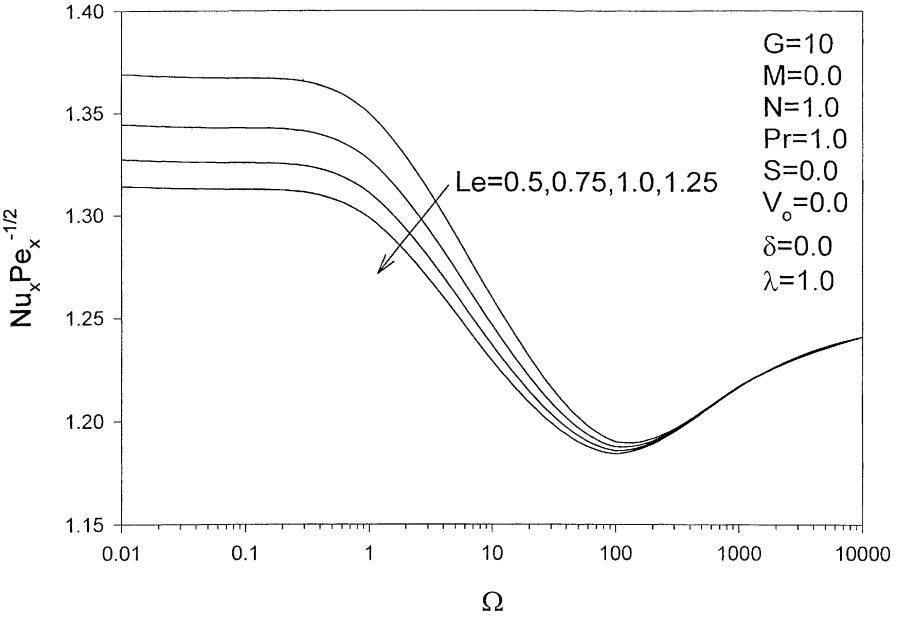

Figure 14.
Effects of Le and Ω on the local Nusselt number

the effect of reducing the fluid linear momentum near the stagnation point. Accordingly, both the skin-friction parameter and the local Nusselt number decrease. Conversely, wall fluid suction produces the opposite effect, namely, increases in both SFP and $Nu_xPe_x^{-1/2}$. These behaviours are depicted in Figures 16 and 17.

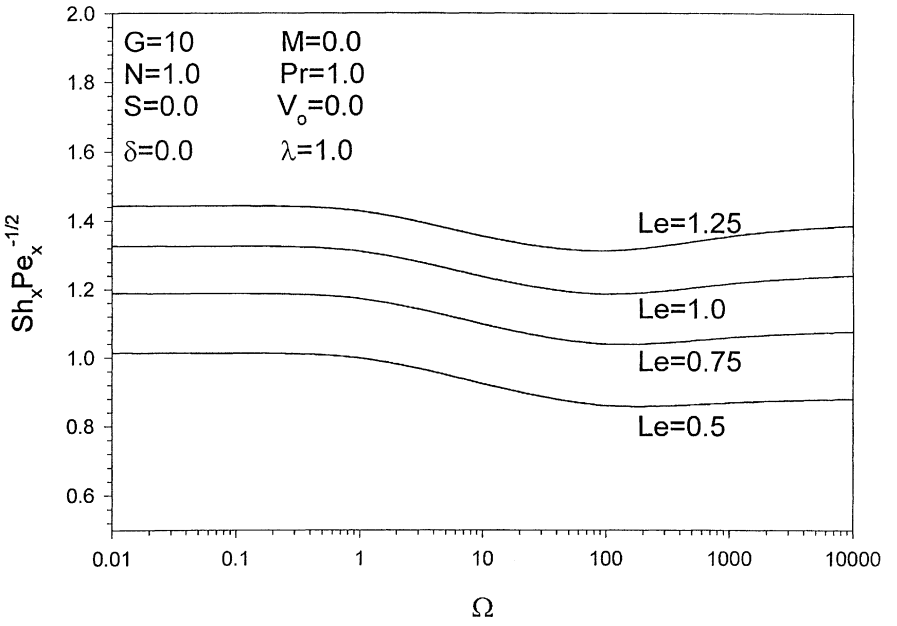

Figure 15.
Effects of Le and Ω on the Sherwood number

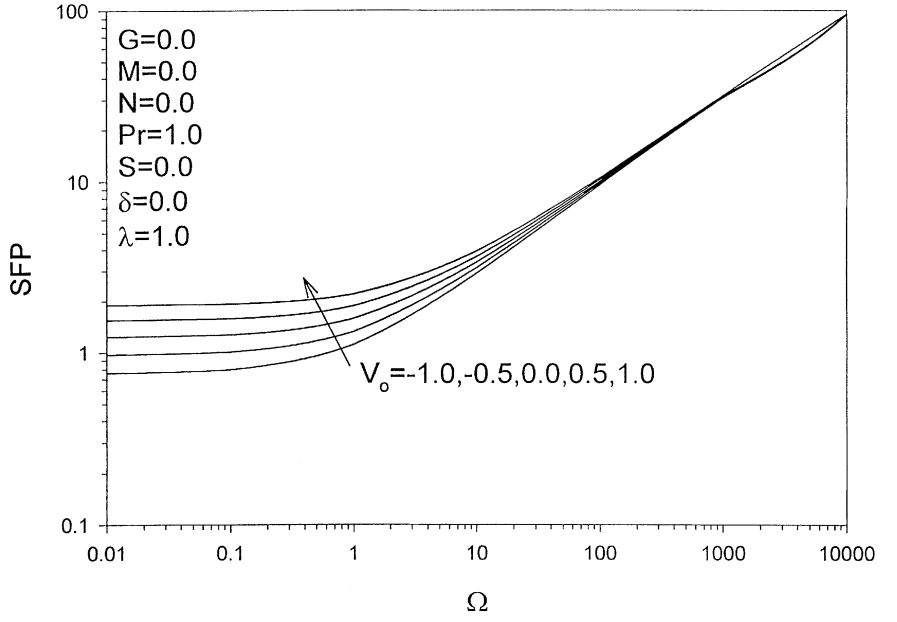

Figure 16.
Effects of V_o and Ω on the skin-friction parameter

Some useful correlations

- The following correlation is obtained for the local Nusselt number as functions of the Prandtl number, dimensionless porous medium

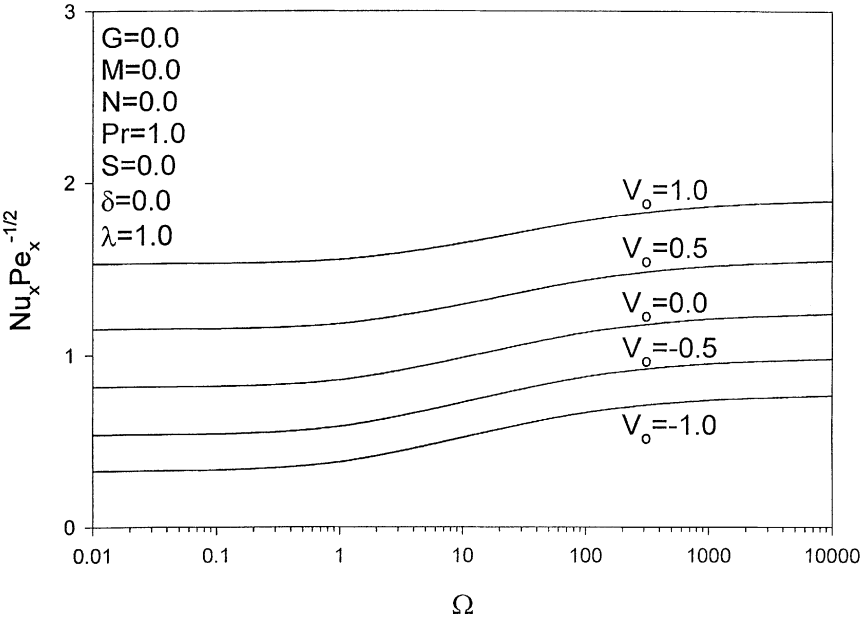

Figure 17.
Effects of V_o and Ω on the local Nusselt number

coefficient Ω and the local Reynold with all of G, M, N, S, V_o and δ are set to zero and λ equal to unity

$$\mathrm{Nu_x} = \frac{1.04804\mathrm{Pr}^{0.4403}\mathrm{Re_x^{0.5}}}{\left(1+\frac{1}{\Omega}\right)^{0.04654}} \tag{24}$$

This correlation gives a maximum error of 9 per cent for the range $10^{-3} < \Omega < 10^2$ and $0.01 < \mathrm{Pr} < 10$. The same can be applied for the case where the magnetic field is present ($\mathrm{M} \neq 0$). This requires the replacement of $1/\Omega$ by $1/(\Omega + \mathrm{M})$ with the range $10^{-3} < \Omega + \mathrm{M} < 10^2$.

- The following correlation is obtained for the local Nusselt number as functions of the dimensionless wall mass transfer coefficient, the dimensionless porous medium coefficient Ω and the local Peclet number with all of G, M, N, S, and δ set to zero and Pr and λ are equal to unity

$$\mathrm{Nu_x} = \frac{0.5184(2+\mathrm{V_0})^{1.1356}\mathrm{Pe_x^{0.5}}}{\left(1+\frac{1}{\Omega}\right)^{0.04828}} \tag{25}$$

This correlation gives a maximum error of 7 per cent for the range $10^2 < \Omega < 10^5$ and $-1.0 < \mathrm{V_o} < 1.0$.

- The following correlation is obtained for the local Nusselt number as functions of the dimensionless internal heat generation or absorption coefficient δ, dimensionless porous medium coefficient Ω and the local Peclet number with all of G, M, N, S, and V_o are set to zero and Pr and λ are equal to unity

$$\frac{Nu_x = 1.5627 Pe_x^{0.5}}{(2+\delta)^{0.4265}\left(1+\frac{1}{\Omega}\right)^{0.0038289}} \quad (26)$$

This correlation gives a maximum error of 3 per cent for the range $10^{-4} < \Omega < 10^5$ and $-1.0 < \delta < 1.0$.

Conclusion

The problem of steady, laminar, hydromagnetic heat and mass transfer by mixed convection boundary-layer flow of an electrically-conducting and heat generating or absorbing fluid near a stagnation point on a vertical permeable semi-infinite plate embedded in a porous medium with power-law variations in both the wall temperature and concentration was considered. The free stream temperature was assumed to be linearly stratified with the vertical distance. The governing equations were developed and transformed using appropriate similarity transformations. The resulting local similarity equations were found to exhibit a self-similar form for a power-law index of unity. The transformed equations were then solved numerically by an implicit, iterative, finite-difference scheme. The obtained results for special cases of the problem were compared with previously published work and were found to be in excellent agreement. It was found that while the local Nusselt number was increased as the Prandtl number, mixed convection parameter, buoyancy ratio or the dimensionless stratification parameter increased. However, it decreased as the dimensionless internal heat generation coefficient or the Lewis number increased when the buoyancy forces were present. The skin-friction parameter was found to increase when both the buoyancy ratio and the dimensionless wall mass transfer increased. In addition, varying the Prandtl number had no effects on the local skin-friction parameter at large values of Ω while it was affected for lower values of Ω. The same was observed when the dimensionless internal heat generation or absorption coefficient was altered. It is hoped that the present work will serve as a vehicle for understanding more complex problems involving the various physical effects investigated in the present problem.

References

Acharya, S. and Goldstein, R.J. (1985), "Natural convection in an externally heated vertical or inclined square box containing internal energy sources", *ASME. J. Heat Transfer*, Vol. 107, pp. 855-66.

Aldoss, T.K., Al-Nimr, M.A., Jarrah, M.A. and Al-Sha'er, B. (1995), "Magnetohydrodynamic mixed convection from a vertical plate embedded in a porous medium", *Numer. Heat Transfer*, Vol. 28A, pp. 635-45.

Ariel, P.D. (1994), "Hiemenz flow in hydromagnetics", *Acta Mech.*, Vol. 103, pp. 31-43.

Blottner, F.G. (1970), "Finite-difference methods of solution of the boundary-layer equations", *AIAA Journal*, Vol. 8, pp. 193-205.

Chamkha, A.J. (1996), "Non-Darcy hydromagnetic free convection from a cone and a wedge in porous media", *Int. Commun. Heat Mass Transfer*, Vol. 23, pp. 875-87.

Chamkha, A.J. (1997a), "MHD-free convection from a vertical plate embedded in a thermally stratified porous medium with hall effects", *Appl. Math. Modelling*, Vol. 21, pp. 603-09.

Chamkha, A.J. (1997b), "Non-Darcy fully developed mixed convection in a porous medium channel with heat generation/absorption and hydromagnetic effects", *Numer. Heat Transfer*, Vol. 32, pp. 853-75.

Chen, T.S. and Yuh, C.F. (1980), "Combined heat and mass transfer in mixed convection along vertical and inclined plates", *Int. J. Heat Mass Transfer*, Vol. 23, pp. 527-37.

Cheng, P. and Minkowycz, W.J. (1977), "Free convection about a vertical flat plate embedded in a porous medium with application to heat transfer from a dike", *J. of Geophy*, Vol. 82, pp. 2040-44.

Eckert, E.R.G. (1942), "Die Berechnung des Wärmeüberganges in der laminaren Grenzschicht umströmter Körper", *VDI Forschungsheft*, VDI, p. 416.

Evans, H.L. (1962), "Mass transfer through laminar boundary layers. 7. Further similar solutions to the b-equation for the case B = 0", *Int. J. Heat Mass Transfer*, Vol. 5, pp. 35-57.

Gebhart, B. and Pera, L. (1971), "The nature of vertical natural convection flows resulting from the combined buoyancy effects of thermal and mass diffusion", *Int. J. Heat Mass Transfer*, Vol. 14, pp. 2025-50.

Hiemenz, K. (1911), "Die Grenzschicht an einem in den gleichförmigen Flüssigkeitsstrom eingetauchten geraden Kreiszylinder", *Dingl. Poltech. J.*, Vol. 326, pp. 321-410.

Kumari, M., Pop, I. and Nath, G. (1985), "Finite difference and improved perturbation solutions for free convection on a vertical cylinder embedded in a saturated porous medium", *Int. J. Heat Mass Transfer*, Vol. 28, pp. 2171-74.

Lai, F.C. (1991), "Coupled heat and mass transfer by mixed convection from a vertical plate in a saturated porous medium", *Int. Commun. Heat Mass Transfer*, Vol.18, pp. 93-106.

Lai, F.C. and Kulacki, F.A. (1990), "The influence of lateral mass flux on mixed convection over inclined surfaces in saturated porous media", *ASME J. Heat Transfer*, Vol. 112, pp. 515-18.

Lin, H.T. and Lin, L.K. (1987), "Similarity solutions for laminar forced convection heat transfer from wedges to fluids of any Prandtl number", *Int. J. Heat Mass Transfer*, Vol. 30, pp. 1111-18.

Minkowycz, W.J. and Cheng, P. (1976), "Free convection about a vertical cylinder embedded in a porous medium", *Int. J. Heat Mass Transfer*, Vol. 19, pp. 508-513.

Pera, L. and Gebhart, B. (1972), "Natural convection boundary layer flow over horizontal and slightly inclined surfaces", *Int. J. Heat Mass Transfer*, Vol. 16, pp. 1131-46.

Raptis, A., Massias, C. and Tzivanidis, G. (1982), "Hydromagnetic free convection flow through a porous medium between two parallel plates" , *Phys. Lett*, Vol. 90A, pp. 288-9.

Sparrow, E.M., Eckert, E.R. and Minkowycz, W.J. (1962), "Transpiration cooling in a magnetohydrodynamic stagnation-point flow", *Appl. Sci. Res.*, Vol. A11, pp. 125-47.

Vajravelu, K. and Nayfeh, J. (1992), "Hydromagnetic convection at a cone and a wedge", *Int. Commun. Heat Mass Transfer*, Vol. 19, pp. 701-10.

Yih, K.A. (1997), "The effect of transpiration on coupled heat and mass transfer in mixed convection over a vertical plate embedded in a saturated porous medium", *Int. Commun. Heat Mass Transfer*, Vol. 24, pp. 265-75.

Yih, K.A. (1998), "The effect of uniform suction/blowing on heat transfer of magnetohydrodynamic Hiemenz flow through porous media", *Acta Mech.*, Vol. 130, pp. 147-58.